Final Scientific/Technical Report (DOE F 241.3)

Report/Product Number: DOE-REDOX-0006735

1. Programmatic Information

Project Title:	Affordable, High-Performance, Intermediate Temperature Solid Oxide Fuel Cells
Project Period:	October 1st, 2014 – March 31st, 2017
Recipient:	Redox Power Systems, LLC 4467 Technology Drive Suite 2107, Bldg 387 College Park, MD 20742
Award Number:	DE-EE0006735
Working Partners:	University of Maryland
Cost-Sharing Partners:	University of Maryland
PI:	Bryan M. Blackburn, Ph.D Phone: 301-314-1959 Email: bryan@redoxenergy.com, bryan@redoxpowersystems.com
DOE Project Team:	DOE Contracting Officer – Lalida Crawford DOE Project Managers – David Peterson, Jacob Spendelow Project Engineer – Shaun Onorato (CNJV)

Acknowledgment: This material is based upon work supported by the U.S. Department of Energy's Office of Energy Efficiency and Renewable Energy (EERE) under the Fuel Cell Technologies Office (FCTO) under Award Number DE-EE0006735.

2. Executive Summary

In this project, we improved the power output and voltage efficiency of our intermediate temperature solid oxide fuel cells (IT-SOFCs) with a focus on ~600 °C operation. At these temperatures and with the increased power density (i.e., fewer cells for same power output), the stack cost should be greatly reduced while extending durability. Most SOFC stacks operate at temperatures greater than 800 °C. This can greatly increase the cost of the system (stacks and BOP) as well as maintenance costs since the most common degradation mechanisms are thermally driven. Our approach uses no platinum group metal (PGM) materials and the lower operating temperature allows use of simple stainless steel interconnects and commercial off-the-shelf gaskets in the stack. Furthermore, for combined heating and power (CHP) applications the stack exhaust still provides "high quality" waste heat that can be recovered and used in a chiller or boiler. The anticipated performance, durability, and resulting cost improvements (< $700/kWe) will also move us closer to reaching the full potential of this technology for distributed generation (DG) and residential/commercial CHP. This includes eventual extension to cleaner, more efficient portable generators, auxiliary power units (APUs), and range extenders for transportation.

The research added to the understanding of the area investigated by exploring various methods for increasing power density (Watts/square centimeter of active area in each cell) and increasing cell efficiency (increasing the open circuit voltage, or cell voltage with zero external electrical current). The results from this work demonstrated an optimized cell that had greater than 1 W/cm^2 at 600 °C and greater than 1.6 W/cm^2 at 650 °C. This was demonstrated in large format sizes using both 5 cm by 5 cm and 10 cm by 10 cm cells. Furthermore, this work demonstrated that high stability (no degradation over > 500 hours) can be achieved together with high performance in large format cells as large as 10 cm by 10 cm when operated at ~600 °C. The project culminated in the demonstration of a 12-cell stack using the porous anode-based SOFC technology.

3. Summary of Accomplishments

All major project objectives were achieved during this development effort. The original approach for this project involved the use of a bilayer electrolyte SOFC design with graded electrode structures. The original development plan focused on the optimization of the gadolinium doped ceria (GDC) and erbia stabilized bismuth oxide (ESB) electrolyte layers, in order to maximize the cell efficiency (increase open circuit potential, or OCP, to a target of > 0.9 Volts) and minimize the electrolyte area specific resistance (ASR) for IT operation (target ASR < 0.2 Ω-cm^2). Additionally, development efforts were focused on using nano-scale catalysts introduced into the anode or cathode using infiltration to increase electrode catalytic/ electrocatalytic activity, which reduces polarization losses and improves cell electrical performance. Development also involved considerable effort to introduce as-processed porosity into the anode support layer (ASL) of unreduced cells in order to gain access to the anode bulk and to the anode-electrolyte interface in order to facilitate infiltration operations. Significant progress was made at the button cell level for both the bilayer electrolyte and the porous anode-based cell. After the Go/No-Go Decision Point, Redox determined that there were too many challenges involved in the scaled-up of the bilayer electrolyte for operation at 600 °C to continue its development in any reasonable amount of time under this project. Therefore, Redox, after discussions with DOE, decided to finish the remainder of the project with a focus on the scale-up of the porous anode support and infiltration efforts while maintaining the same project goals.

Major achievements during this development project are summarized below:

- Achieved an OCP of 0.93 V (target: > 0.9 V), maximum power density of 1.27 W/cm^2 (target: > 1 W/cm^2), and an ASR of 0.171 Ω-cm^2 (target: < 0.2 Ω-cm^2) at 600 °C using infiltrated porous anode-based button cells with the bilayer electrolyte;

- Achieved an OCP of 0.91 V (target: > 0.9 V) using one of Redox's 10 cm by 10 cm production cells with a bilayer electrolyte;

- Demonstrated stable interconnect coatings and contact materials with combined ASR as low as 0.052 Ω-cm^2 at 600 °C (target: ASR ≤ 0.15 Ω-cm^2);

- Achieved > 0.88 V OCP (target: ~0.9 V) using a 10 cm by 10 cm porous anode-based cell with a single GDC electrolyte, which was an ~13% increase over non-infiltrated cell with an equivalent electrolyte thickness;

- Achieved ASR ≤ 0.2 Ω-cm^2 at 600 °C using an optimized 10 cm by 10 cm large format, porous anode-based SOFC;

- Achieved > 1 W/cm^2 at 600 °C and achieved power density of > 1.6 W/cm^2 at 650 °C using 5 cm by 5 cm porous-anode cells in humidified hydrogen fuel;

- Demonstrated stability of optimized porous anode-based SOFC (5 cm by 5 cm) at 600 °C and 1.3 A/cm^2 in humidified hydrogen fuel for over 500 hours with *no* degradation (target: degradation ≤ 2% per 1,000 hours);

- Demonstrated that there was no sign of phase change or morphology change (e.g., densification) in anode support scaffold or infiltrate after more than 1,000 hours of testing of porous anode-based cell between 600 °C and 650 °C; and

- Demonstrated a 12-cell stack using 5 cm by 5 cm porous anode-based SOFC stack tests with performance comparable to 10 cm by 10 cm and 5 cm by 5 cm single cell tests, demonstrating scalability.

4. Summary of Project Activities and Results

In this project, we worked to improve the performance of our intermediate temperature solid oxide fuel cells (IT-SOFCs) focused on ~600 °C operation. At these temperatures, the stack cost should be greatly reduced while significantly extending durability since degradation mechanisms are typically temperature driven phenomena. The anticipated performance, durability, and resulting cost improvements (< $700/kWe) will also move us closer to reaching the full potential of this technology for distributed generation (DG) and residential/commercial CHP.

The objective of the proposed project was to improve performance/durability of our technology through

- *the development of an optimized large format cell (target size: 10 cm by 10 cm) with increased open circuit potential (OCP) and thus greater fuel efficiency for ~600 °C operation;*
- *the optimization of compositions and microstructures of cell electrodes to increase power density for ~600 °C operation; and*
- *the optimization and demonstration of a stack (target size: 100 W up to 1,000 W) using the optimized large format cell at ~600 °C and the creation of cell performance maps.*

The original approach for this project involved the use of a bilayer electrolyte SOFC design with graded electrode structures. The original development plan focused on the optimization of the *total bilayer electrolyte thickness* and *relative thickness* of gadolinium doped ceria (GDC) and erbia stabilized bismuth oxide (ESB) electrolyte layers, in order to maximize the cell efficiency (increase OCP to target of > 0.9 Volts) and minimize the electrolyte area specific resistance (ASR) for IT operation (target ASR < 0.2 Ω-cm^2). Furthermore, the project was focused on increasing power density (and thus major cost reductions) through optimization of compositions and microstructure of the SOFC electrodes. Lower temperature operation provides a major opportunity to employ submicron, nano-scale catalysts in the electrodes to increase specific surface area and catalalytic/electrocatalytic activity of electrode functional layers. This effectively reduces polarization losses and improves electrical performance. Catalysts are introduced into the electrodes via an infiltration process. For anode supported cells, the anode must be porous enough to accept the infiltrated catalyst. Porous anode development efforts were focused on the use of pore formers to introduce porosity into the anode support layer (ASL) of unreduced cells without sacrificing cell strength, so that catalysts can be subsequently infiltrated to enhance cell performance and so that the cells can be assembled in a stack.

At the Go/No-Go point in the project, we had successfully adjusted the relative and total GDC/ESB bilayer thickness to improve the cell OCP above the target value. Figure 1A shows the typical microstructure for a button cell with the bilayer electrolyte. For the bilayer button cell optimization process the GDC thickness was varied between ~12 microns and ~40 microns, while the ESB thickness was kept between ~5-20 microns. The cells were tested in a standard button cell reactor with a ceramic cement based sealant using humidified hydrogen and air.

Figure 1B shows the OCP at different temperatures (500-650 °C) for a bilayer electrolyte cell and a GDC-only electrolyte cell. In these cases the GDC layer was ~20 microns for both cells, while the bilayer cell additionally had an ESB layer that was ~4 microns thick. There was an approximately 40 mV increase in OCP at each temperature, which can translate to a gain in cell efficiency for operating temperatures ≤ 600 °C.

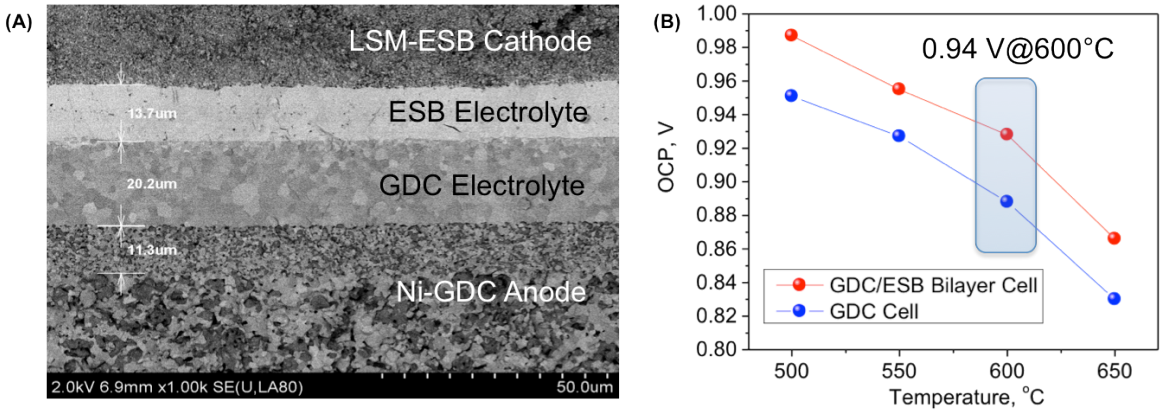

Figure 1. Button cell bilayer electrolyte cell results with (A) an SEM cross-section displaying the typical microstructure, and (B) OCP results for a bilayer electrolyte cell versus a GDC-only electrolyte cell from 500 °C to 650 °C.

Figure 2 compares the performance of a conventional bilayer electrolyte button cell with two porous anode-based cells that had different infiltrated catalysts as well as the bilayer electrolyte. Using these cells we successfully demonstrated a bilayer button cell operating on humidified hydrogen fuel and air (1 atm) with an OCP as high as 0.94 V at 600 °C. As shown in Figure 2, we also demonstrated a button cell with an OCP of 0.93 V at 600 °C and a maximum power density of 1.27 W/cm^2. The cell also had an ASR of 0.171 Ω-cm^2.

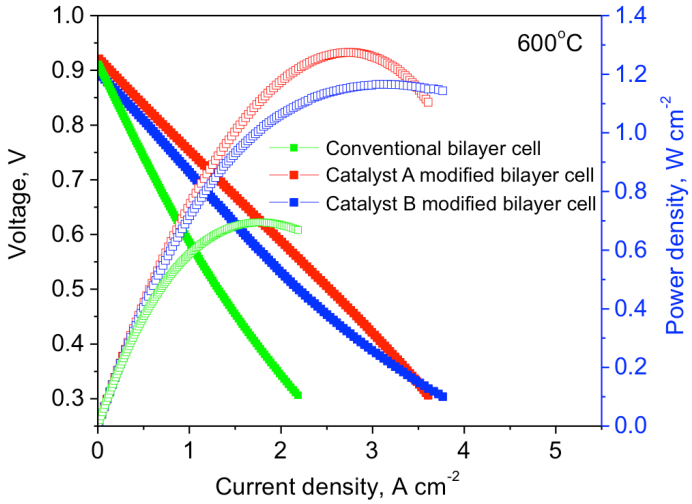

Figure 2. Button cell results demonstrating bilayer electrolyte cell power density of ~1.27 W/cm^2 with an OCP of 0.93 V using humidified H_2 at ~600 °C.

To assist in the development of cells and stacks for operation at ~600 °C, Redox made use of our advanced multi-physics model, which takes into account the unique thermochemical and physical properties of the Redox materials. This is critical due to variations in conductivity and chemical activity of GDC as a function of temperature and effective oxygen partial pressure P_{O2}, which varies significantly down the channel in SOFC anodes with increasing fuel utilization (Figure 3).

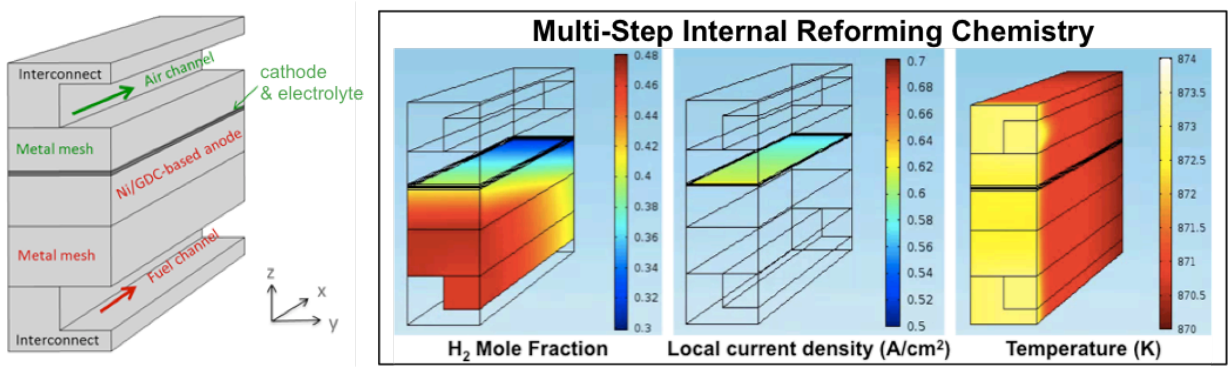

Figure 3. Example output of multi-physics, single channel model which captures thermochemistry and various aspects of Redox's unique cell materials set.

Redox integrated the physics of the GDC/ESB bilayer into our custom single-channel SOFC multiphysics model. The bilayer model employs SOFC layers consisting of Ni-GDC or Ni-YSZ anodes, GDC and ESB bilayer electrolytes, and an LSM-ESB cathode. We used the model to simulate both button cells and stack components with outputs consisting of polarization curves, 3-D temperature profiles, and composition distribution based on temperature dependent input kinetic parameters and electrical properties associated with the electrolyte and electrode materials. The bilayer model parameters were fit to the button cell data at 600 °C, and validated by correctly predicting performance at 650 °C (Figure 4). The only change made to the model input during validation was the operating temperature, which demonstrates that the charge-transfer reaction rate expressions and proposed kinetic parameters are adequate to predict the GDC/ESB bilayer cell performance under different conditions. This has also been confirmed with different data from higher temperatures and predicting performance at lower temperatures, as well as with isothermal conditions for variations in the ESB and GDC thickness. The model also captures the kinetics of electrochemical and heterogeneous internal reforming reactions in the anode, and therefore now represents a complete multi-physics tool for cell/stack investigations.

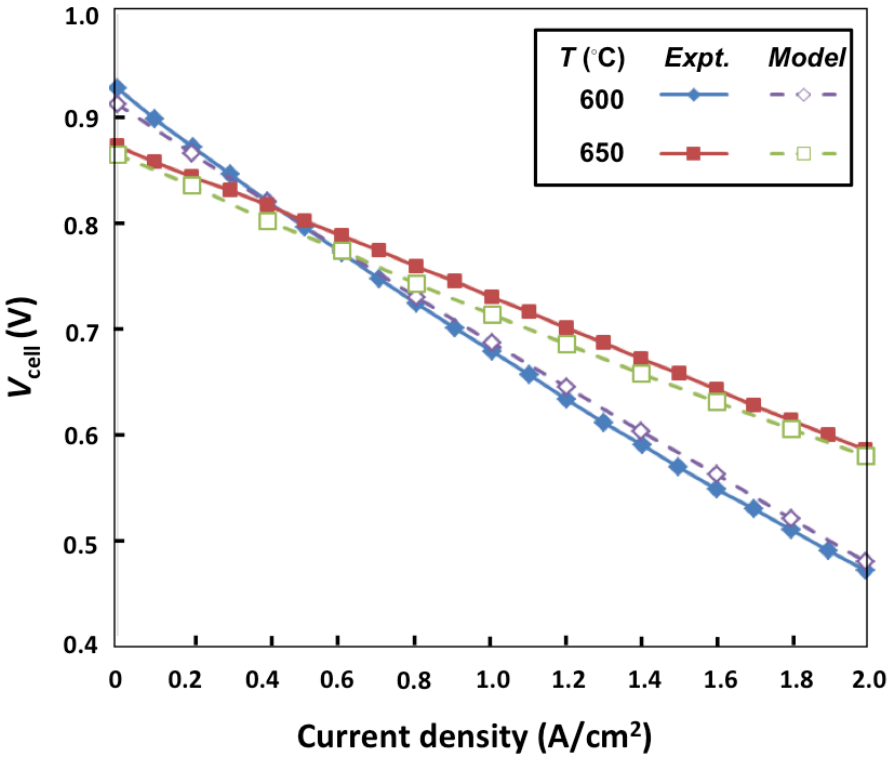

Figure 4. Comparison of simulated electrochemical performance of the bilayer cell versus experimental I-V curves at 600 °C and 650 °C.

At the time of the Go/No-Go decision point, the porous anode-based cell was still undergoing the scale-up process. Therefore, we used standard Redox production cells to scale-up the bilayer electrolyte configuration to the 10 cm by 10 cm size. These cells had a denser ASL into which infiltration was not possible. As shown in Figure 5, we demonstrated a 10 cm by 10 cm ESB/GDC bilayer electrolyte cell exhibiting an OCP of 0.91 V at ~600 °C. This demonstration was achieved by the integration and scaling of earlier project efforts and deliverables from the button cell level. While this was higher than the target OCP (≥ 0.9 V), the value was lower than what was achieved for the button cells (as high as 0.94 V). Our multi-physics model predicted that this was due in part to an undesirable porosity in the ESB layer for the 10 cm by 10 cm cell, which could have caused a decreased conductivity and/or reduced triple phase boundary (TPB). This can result in a lower OCP due to the mixed electronic and ionic conductivity in the GDC layer.

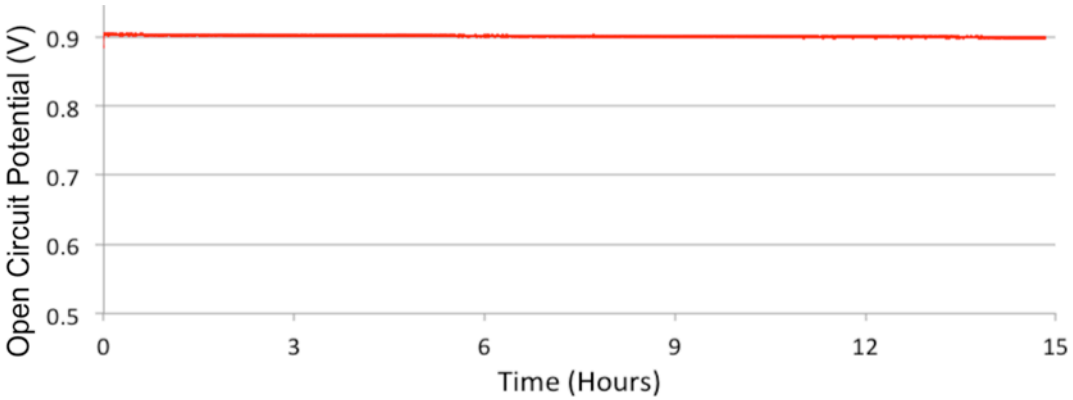

Figure 5. OCP for Redox 10 cm by 10 cm production cell tested at ~600 °C in H_2.

Figure 6A shows the microstructure of the ESB layer for the button cell which was sintered at temperature T1. Figure 6B and 6C show the microstructure for a 10 cm by 10 cm cell sintered at T1 and T2, respectively, where T1 > T2. Due to furnace temperature gradients, the 10 cm by 10 cm cell whose results are shown in Figure 5 was actually fired at T2 even though the furnace setpoint was the same as in the button cell fabrication. When the furnace was adjusted so the actual temperature was T1, the larger size cell still was denser but still more porous than the button cell. After many attempts to optimize the microstructure of the ESB layer in the larger format cells, a decision was made, after discussions with DOE, to focus solely on achieving the project objectives using the infiltrated porous anode-based cell possessing only a single GDC electrolyte.

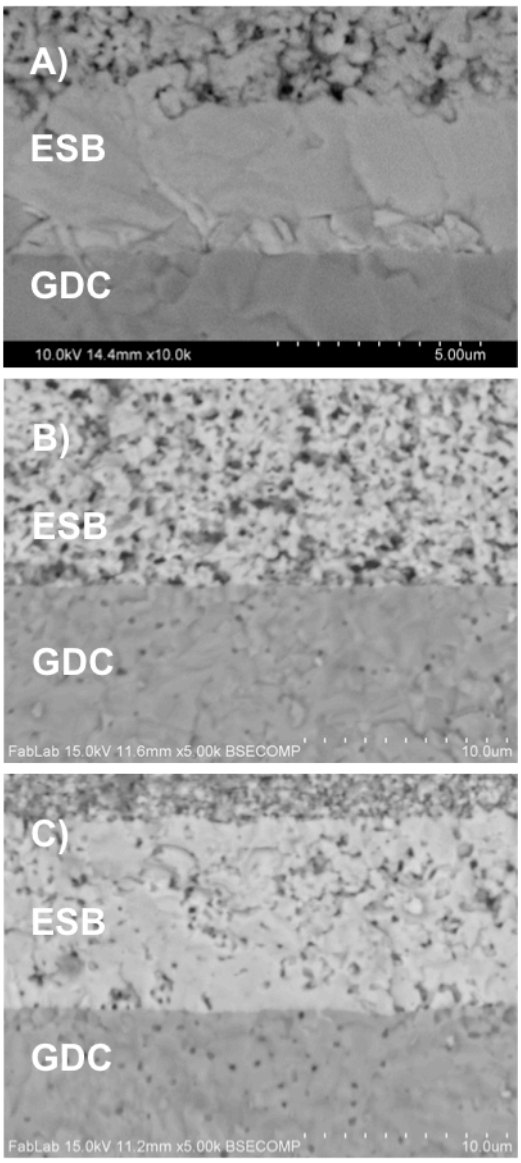

Figure 6. SEM cross-sections comparing ESB microstructure for (A) a button cell sintered at T1, (B) a 10 cm by 10 cm cell fired at T2 < T1, and (C) a 10 cm by 10 cm cell fired at T1.

Figure 7 compares the microstructure results of a first attempt at a scaled-up porous anode-supported 10 cm by 10 cm cell and a more optimized version. The half cells utilized tape cast layers made in a production environment. As seen in Figure 7A, the initial cells had a great deal of closed porosity in the anode support layer (ASL) and a dense anode functional layer (AFL). In order to gain a more interconnected pore network we used a broader particle size distribution for the pore former. We also made a porous AFL (Figure 7B), which together with the optimized ASL resulted in a microstructure that was very similar to those of the porous anode-supported button cells used to achieve 1.27 W/cm^2 at ≤ 600 °C in Figure 2.

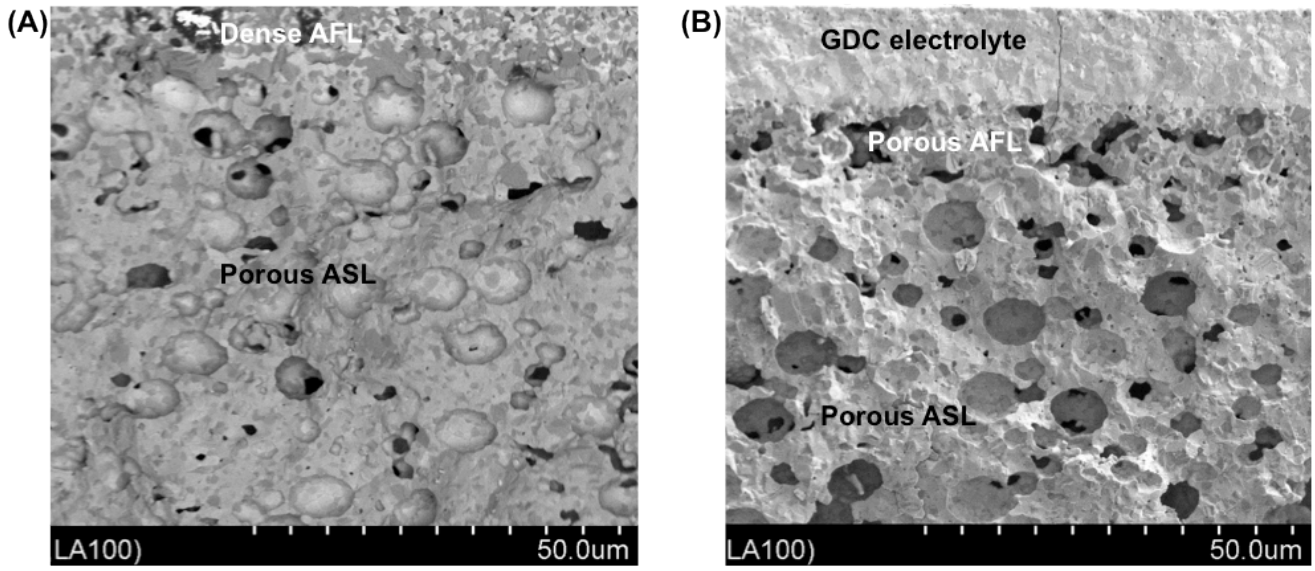

Figure 7. SEM cross-sections comparing microstructure of production manufactured, porous anode-supported cells using (A) original and (B) an optimized scaled-up tape materials.

For the initial electrical characterization testing, porous anode-based cells with infiltrated cathodes and anodes were fabricated at the 5 cm by 5 cm size and tested using humidified hydrogen between ~600 °C and 650 °C. As shown in Figure 8, at 650 °C the maximum power density was ~1.6 W/cm^2. The performance at ~600 °C was also quite impressive with performance greater than 1 W/cm^2. We anticipate that with a slight increase in GDC thickness, the OCP of the porous anode-based cells can be increased further without much negative impact on power density at ~600 °C. There are some slight non-linear behavior in the voltage-current characteristic. Figure 8 also shows performance at ~625 °C, which had a maximum power density of ~1.3 W/cm^2. The OCP at ~600 °C for the infiltrated porous anode-based cell was ~0.88 V (an approximately 13% increase over non-infiltrated cell with an equivalent electrolyte thickness). While this falls slightly under the target OCP of 0.90 V and the 0.94 V that was achieved with the bilayer button cells, the thickness of the GDC for the porous anode-cells was much less than that of the bilayer cells. We believe the OCP can be increased with a slightly thicker GDC layer for the porous anode-based cell without jeopardizing the power density at ~600 °C.

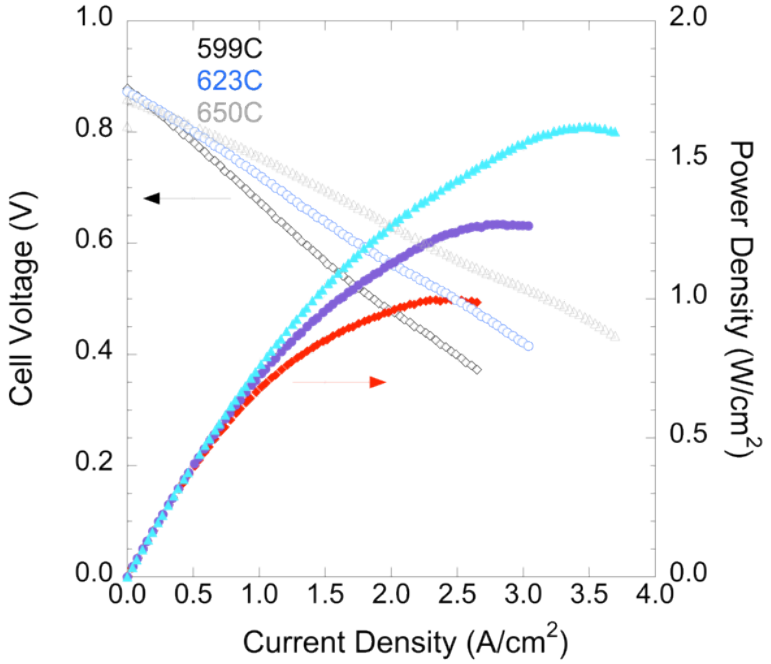

Figure 8. Voltage and power density as a function of current density for a 5 cm by 5 cm porous anode-based cell tested between ~600 °C and ~650 °C showing the achievement of more than 1 W/cm^2 at 600 °C and more than 1.6 W/cm^2 at 650 °C.

After the initial characterization of the single 5 cm by 5 cm porous anode-based cell between 600 °C and 650 °C, the cell was tested for long-term durability at 600 °C under constant current. The cell was held constant at 600 °C under 1.3 A/cm^2 constant load for more than 500 hours. The long-term voltage stability versus time is shown in Figure 9. The occasional increase in cell voltage was when current density was briefly brought to zero to assess OCP stability and to allow impedance spectroscopy measurements to be taken. Rather than experiencing degradation, the OCP and power density actually increased slightly over time, the latter increasing by ~2% over the 500 hours. Area specific resistance (ASR) also exhibited similar behavior, with ASR improving by ~6% over time. After long-term testing of the cell at 600 °C, it was subsequently tested for close to an additional 500 hours at 650 °C before being cooled to room temperature. Post-test X-ray diffraction characterization of the anode support revealed no phase change within porous anode during testing.

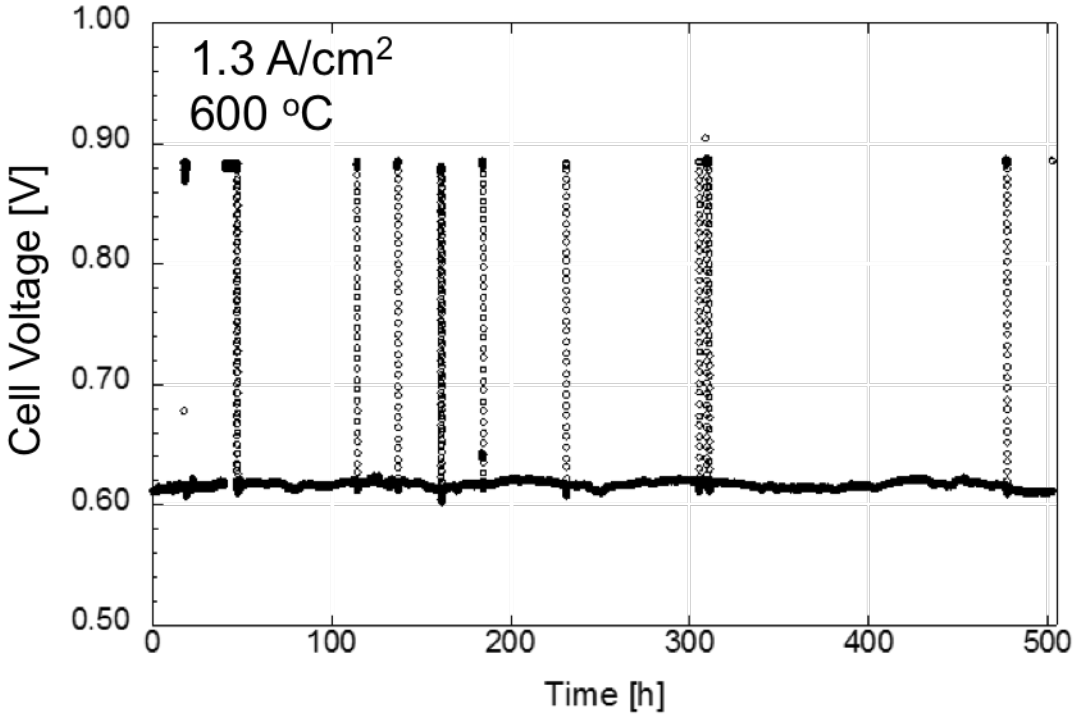

Figure 9. Long-term performance of 5 cm by 5 cm porous anode-based cell operating at 1.3 A/cm^2 and 600 °C.

In order to understand the origin of long-term degradation, or performance improvement, impedance spectroscopy is often performed to separate ohmic from non-ohmic (electrode reaction) contributions. The impedance spectra for the 5 cm by 5 cm single cell described above can be found in Figure 10 (legend reports hours into measurement at 600 °C). The measurement was carried out close to open circuit conditions. The total resistance of the cell, given by the low frequency intercept with the x-axis (right-most points in Figure 10) is equivalent, within experimental error, to the resistance extracted from I-V data in Figure 8 near open circuit conditions, confirming good agreement between the techniques. The width of the flattened semi-circle in the figure represents the non-ohmic portion of the cell resistance. As time progresses from 0 to 433 hours, the width of the semi-circle remains largely the same, while the high frequency intercept (most left point), representing the ohmic contribution, decreases. The first key interpretation of this result is that despite long-term operation, the electrode reactivity remains the same, indicating that there is no degradation of infiltrate at this operating condition for more than 400 hours. The second key interpretation from the impedance spectra results is that an ohmic contribution is improving with operation, and this could very likely be related to a decrease in a contact resistance and/or current collection capability as the electrolyte is not expected to age. Together with the voltage stability data collected over more than 500 hours, we have demonstrated that our optimized porous anode-based cells are very stable and far exceed the project target of ≤ 2% degradation per 1,000 hours (tested over ≥ 300 hours).

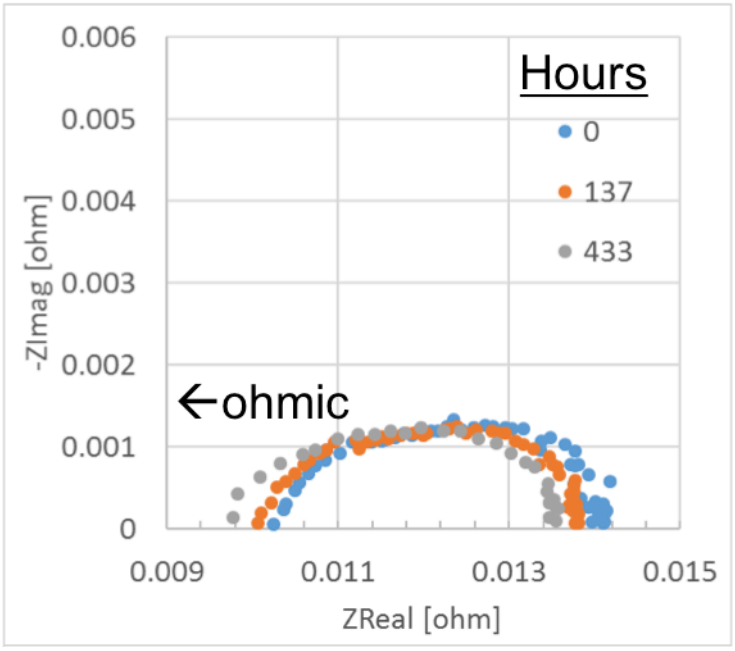

Figure 10. Impedance spectra collected around open circuit voltage for 5 cm by 5 cm porous anode-based cell operated at 600 °C for 500 hours at ~1.3 A/cm^2.

Consistent with the long-term stability in electrical characteristics, Figure 11 shows a SEM image of an intentionally fractured surface of porous anode composite scaffold from the cell used in durability testing. The image demonstrates that the infiltrated catalyst is able to retain a fine structure after ~1,000 hours of operation over 600 °C to 650 °C. This is significant because the catalyst contributes significantly to the performance enhancements in OCP and power density and matches the conclusions from the electrical characterization and XRD results.

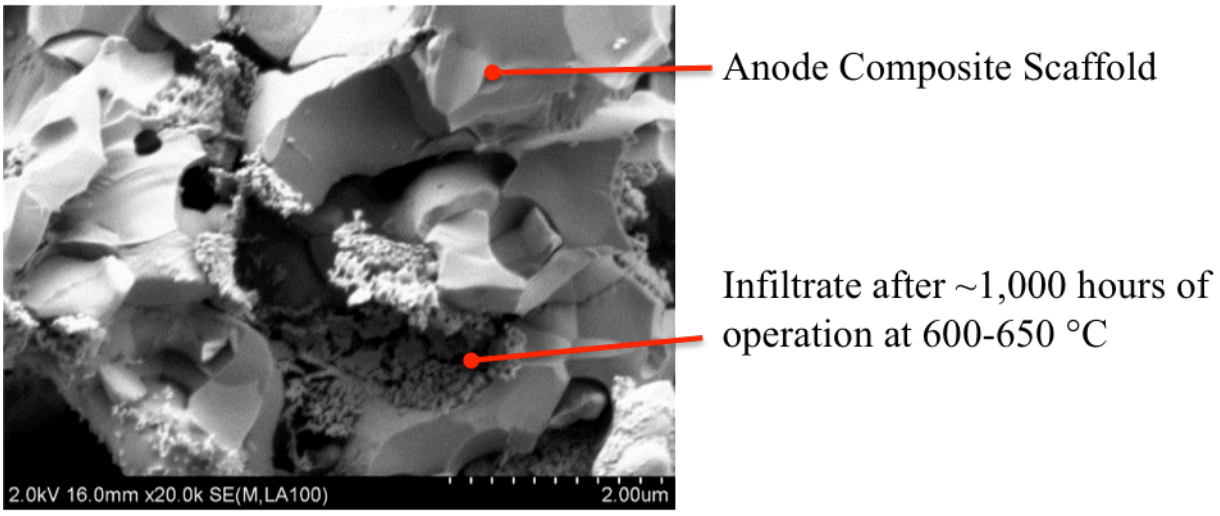

Figure 11. SEM image of intentionally fractured surface of porous anode composite scaffold showing microstructure of infiltrate after 1,000 hours operation at 600 °C to 650 °C.

After having successfully demonstrated the results summarized in Figure 8 through Figure 11 at the 5 cm by 5 cm size, Redox successfully scaled the porous anode-based cells to the 10 cm by 10 cm size. The larger cells were acceptably flat and were made reproducibly in-house as well as with our production firing partner. Figure 12 shows a voltage-current and power density characteristic for a 10 cm by 10 cm porous anode-based cell at ~600 °C and compares the performance to the 600 °C characteristic for the 5 cm by 5 cm cell. The electrical performance of the 10 cm by 10 cm cell is very similar to that of the 5 cm by 5 cm cell at 600 °C. Note that the largest power density in Figure 12 is just over 0.6 W/cm^2, while that in Figure 6 is > 1 W/cm^2. This is because the largest power density in Figure 10 does not represent the maximum power density of the 10 cm by 10 cm cell. At the time of testing for this 10 cm by 10 cm cell, the maximum current carrying capacity had been reached for the power bus cables to the electronic load equipment. However, since the two plots in Figure 12 are at the same scale, it can be seen that the performance of the 5 cm by 5 cm and 10 cm by 10 cm porous anode-based cells is nearly identical. Both the 5 cm by 5 cm cell and the 10 cm by 10 cm cells have an ASR < 0.2 Ω-cm^2 at ~600 °C.

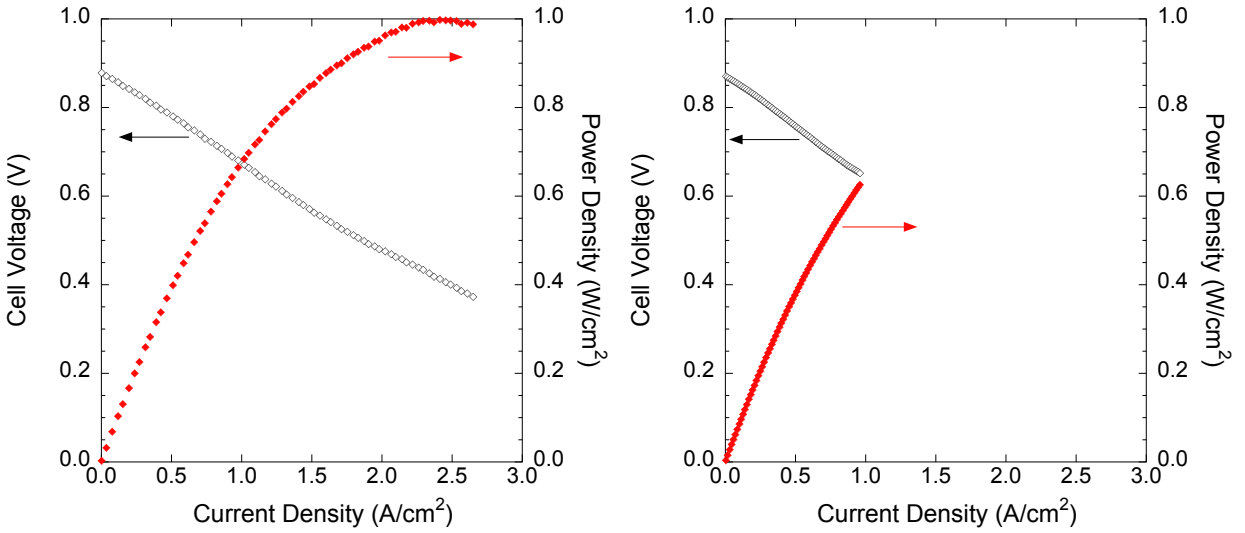

Figure 12: At ~600 °C the voltage and power density are shown as a function of current density for the 5 cm by 5 cm porous anode-based cell (left) and the 10 cm by 10 cm porous anode-based cell (right).

We assembled and tested a 12-cell stack consisting of 5 cm by 5 cm porous anode-based cells. The current-voltage and power characteristics of the stack are shown in Figure 13. The largest average power density of the cells was around 0.65 W/cm^2 at 600 °C. The average ASR was around 0.22 Ω-cm^2 as with the single cell tests at the 5 cm by 5 cm and 10 cm by 10 cm size. The average OCP per cell (~0.83 V) in the 12-cell stack was lower than in the single cell tests, but we believe this had to do with temperature gradients within the stack. Some of the cells had an OCP as high as ~0.85 V and managing the average temperature of the stack was difficult given the power density of the cells under test. The spread in temperatures is what we believe

caused the average ASR to be a little higher than in the single cell tests. We believe that with further optimization the cell performance within a larger stack such as this can be brought closer to the single cell performance level. Overall, the stack test did demonstrate that lower ASRs are possible in relatively large stacks at ~600 °C and did show the promise of our porous anode-based SOFC technology.

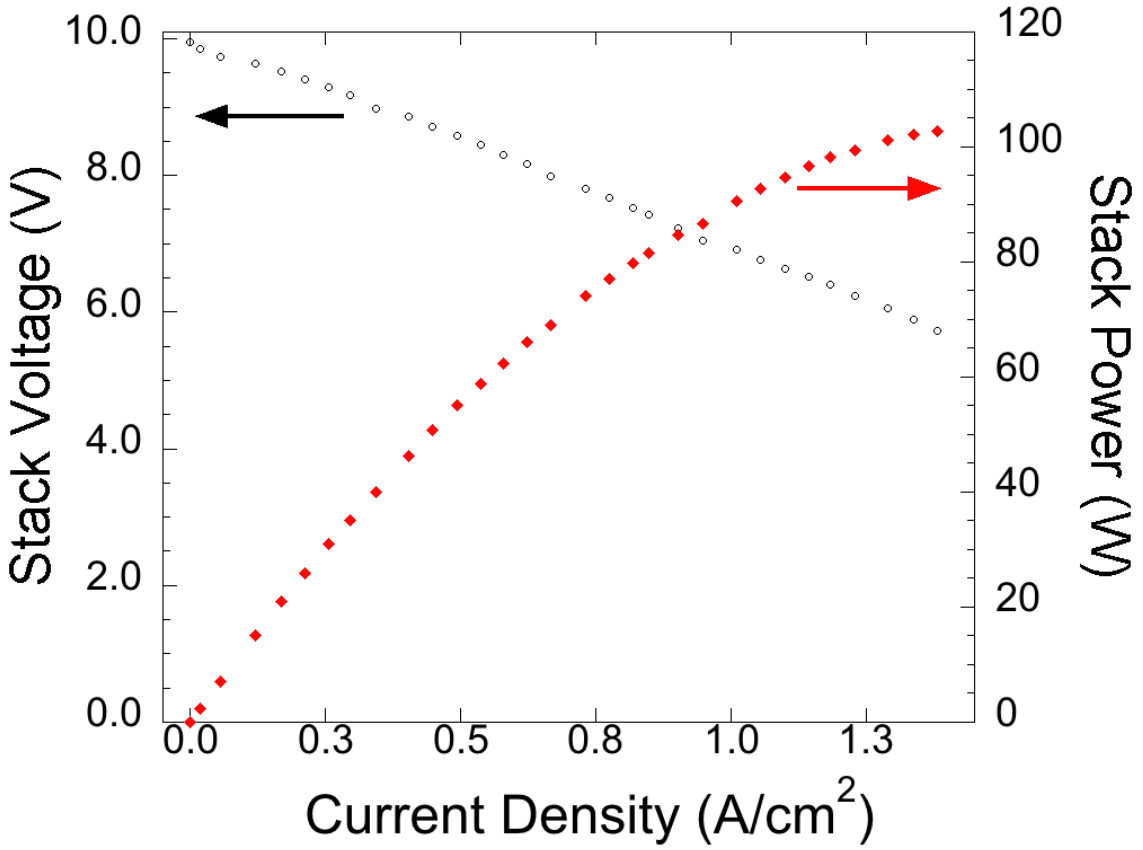

Figure 13. Current-Voltage and stack power characteristic for a 12-cell stack using 5 cm by 5 cm porous anode-based cells.

In addition to the results presented above, Redox optimized a manganese cobalt oxide (MCO) protective coating process for the cathode side of stainless steel stack interconnect. Most of the previous work around MCO-based coatings has been focused on higher operating temperatures (e.g., > 800 °C). In this project, the target performance for the interconnect coating was an ASR less than or equal to 0.15 Ω-cm^2 at 600 °C. Work primarily centered on processing and geometry optimization and characterization of resulting test coupons before scaling the process to full-size interconnects. Films were deposited using an optimized spraying process and heat treatment. During process optimization, film adhesion was determined using Standard Test Methods for Measuring Adhesion by Tape Test (ASTM Standard D3359-09).

Ultimately, we were able to produce MCO coatings with an ASR of 52 milliohm-cm^2 at 600 °C and 13 mohm-cm^2 at 800 °C (Figure 14), which was much better than the targeted performance. For comparison, the performance at 800 °C is similar to reported values in the literature. For example, PNNL has reported an MCO coating with an ASR of 13-17 milliohm-cm^2 at 800 °C (PNNL Report 15303, 2005).

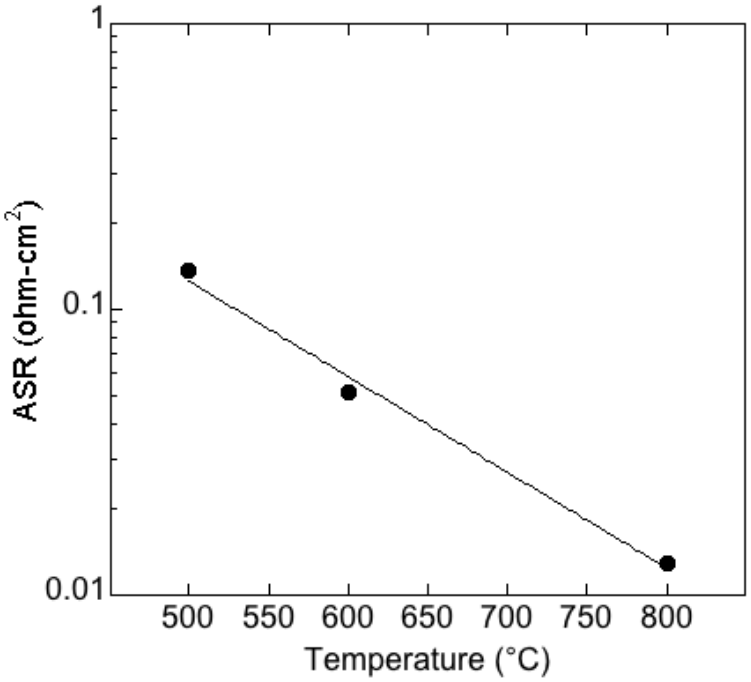

Figure 14. Temperature dependence of ASR for an optimized MCO interconnect coating.

5. Work Product Developed Under The Award & Technology Transfer Activities

a. Publications (list journal name, volume, issue), conference papers, or other public releases of results.

Date	Type	Other Information
06-11-2015	Presentation, publication	Annual Merit Review meeting (Bryan Blackburn)
06-09-2016	Presentation, publication	Annual Merit Review meeting (Bryan Blackburn)
06-05-2017	Poster	Annual Merit Review meeting (Bryan Blackburn)
06-12-2017	Presentation	Annual NETL SOFC meeting (Sean Bishop)
10-04-2017	Presentation	Electrochemical Society Conference (Sean Bishop)

b. Web site or other Internet sites that reflect the results of this project;
N/A

c. Networks or collaborations fostered;
N/A

d. Technologies/Techniques;
N/A

e. Inventions/Patent Applications, licensing agreements; and
Invention: high power porous anode-based SOFC that was developed under this project.

f. Other products, such as data or databases, physical collections, audio or video, software or netware, models, educational aid or curricula, instruments or equipment.
N/A